

Quantitative analysis of ferroelectric domain imaging with piezoresponse force microscopy

Tobias Jungk, Ákos Hoffmann, and Elisabeth Soergel

Citation: *Appl. Phys. Lett.* **89**, 163507 (2006); doi: 10.1063/1.2362984

View online: <http://dx.doi.org/10.1063/1.2362984>

View Table of Contents: <http://apl.aip.org/resource/1/APPLAB/v89/i16>

Published by the [American Institute of Physics](#).

Additional information on *Appl. Phys. Lett.*

Journal Homepage: <http://apl.aip.org/>

Journal Information: http://apl.aip.org/about/about_the_journal

Top downloads: http://apl.aip.org/features/most_downloaded

Information for Authors: <http://apl.aip.org/authors>

ADVERTISEMENT



HAVE YOU HEARD?

Employers hiring scientists
and engineers trust
physicstodayJOBS



<http://careers.physicstoday.org/post.cfm>

Quantitative analysis of ferroelectric domain imaging with piezoresponse force microscopy

Tobias Jungk,^{a)} Ákos Hoffmann, and Elisabeth Soergel

Institute of Physics, University of Bonn, Wegelerstraße 8, 53115 Bonn, Germany

(Received 14 July 2006; accepted 30 August 2006; published online 18 October 2006)

The contrast mechanism for ferroelectric domain imaging via piezoresponse force microscopy (PFM) is investigated. A vectorial description of PFM measurements is presented which takes into account the background caused by the experimental setup. This allows a quantitative, frequency independent analysis of the domain contrast which is in good agreement with the expected values for the piezoelectric deformation of the sample and satisfies the generally required features of PFM imaging. © 2006 American Institute of Physics. [DOI: 10.1063/1.2362984]

Domain engineering in ferroelectric crystals is of increasing importance for nonlinear frequency converters using quasi-phase-matching,¹ photonic crystals,² and ultrahigh density data storage devices.³ Among the techniques utilized for the visualization of ferroelectric domains⁴ piezoresponse force microscopy (PFM) has become a standard tool because of its nondestructive imaging capability with high lateral resolution.⁵ The piezoresponse force microscope is a scanning force microscope operated in contact mode with an additional alternating voltage applied to the tip. In piezoelectric samples this voltage causes thickness changes and therefore vibrations of the surface which lead to oscillations of the cantilever that can be read out with a lock-in amplifier. However, although widely used, the contrast mechanism for domain detection with PFM is still under discussion mainly because of inconsistencies of the measured data regarding the following features:

- (1) Frequency dependence: the domain contrast should be independent of the frequency ω of the alternating voltage applied to the tip (if ω is in the kilohertz range and far away from the resonance frequencies of the cantilever).
- (2) Vibration amplitude: the vibration amplitude Δt of antiparallel domains must be equal, and $\Delta t = dU$ with d being the appropriate piezoelectric constant and U the voltage applied to the tip.⁶
- (3) Phase shift: a phase shift of 180° between the piezoelectric response from antiparallel domains is mandatory.

However, frequency scans of the alternating voltage are reported to show a complex spectrum, i.e., the measured domain contrast strongly depends on the frequency. The vibration amplitudes are not equal on antiparallel domains and the reported values differ by orders of magnitude. A phase difference of 180° is not generally obtained (see, e.g., Refs. 7–13).

Numerous approaches for explaining these inconsistencies have been reported;^{14–16} however, a full quantitative analysis of PFM imaging is still lacking. Although there is no doubt that PFM imaging is sensitive to ferroelectric domains, there is no unambiguous evidence that a contrast in PFM images proves the existence of ferroelectric domains. In this contribution we present a vectorial analysis of the data acquired with PFM. This allows a clear understanding of the

contribution of the converse piezoelectric effect which fully satisfies the features listed above.

For the investigations we used a conventional experimental setup with a commercial scanning force microscope (SMENA, NT-MDT), modified to allow application of voltages to the tip. We utilized different cantilevers (C_1 – C_4) with Ti–Pt coated tips (MikroMasch) of 100–130 μm length, stiffness of 3–70 N/m, and resonance frequencies >150 kHz. For PFM operation we applied an alternating voltage of $10 V_{pp}$ to the tip and detected the resulting oscillation of the cantilever with a lock-in amplifier (SRS 830); the phase being set to 0° and the time constant to 10 ms. We simultaneously recorded the in-phase ($\theta=0^\circ$) output X and the orthogonal ($\theta=90^\circ$) output Y with θ denoting the phase with respect to the driving voltage. In the following these signals will be named PFM signals: **P** on a positive $+z$ domain and **N** on a negative $-z$ domain face, respectively. The sample was a z -cut periodically poled LiNbO₃ (PPLN) crystal ($15 \times 16 \times 0.5 \text{ mm}^3$) periodically poled with a period length of 8 μm .

The experimental procedure was as follows. We first recorded a PFM image of the sample in order to subsequently position the tip accurately on a $+z$ or a $-z$ domain. Then we measured the oscillation amplitude of the cantilever while sweeping the frequency of the alternating voltage from 10 to 100 kHz. The curves shown in this contribution are averages over three frequency scans taken at different positions on the sample surface.

Figure 1 shows frequency scans of the X signal on a $-z$ domain face for four different cantilevers. The frequency spectra look apparently random, although some specific features recur (e.g., at ~ 22 kHz and at ~ 29 kHz for C_1 and C_3 and at ~ 84 kHz for C_1 and C_2). The signal reaches values up to 250 pm whereas only 81 pm are predicted by the converse piezoelectric effect. Moreover, at specific frequencies, no PFM signal is measured and even negative values are obtained. The orthogonal Y signal shows a similar behavior, however, with completely different spectra. Taking into account the required features for PFM imaging listed above, this indicates that only a part of the PFM signal can be attributed to the ferroelectric properties of the sample, the PFM signal being dominated by a complex background signal.

This background signal was determined by averaging the signals from the $+z$ and $-z$ domain faces: $\mathbf{B} = \frac{1}{2}(\mathbf{P} + \mathbf{N})$, there-

^{a)}Electronic mail: jungk@uni-bonn.de

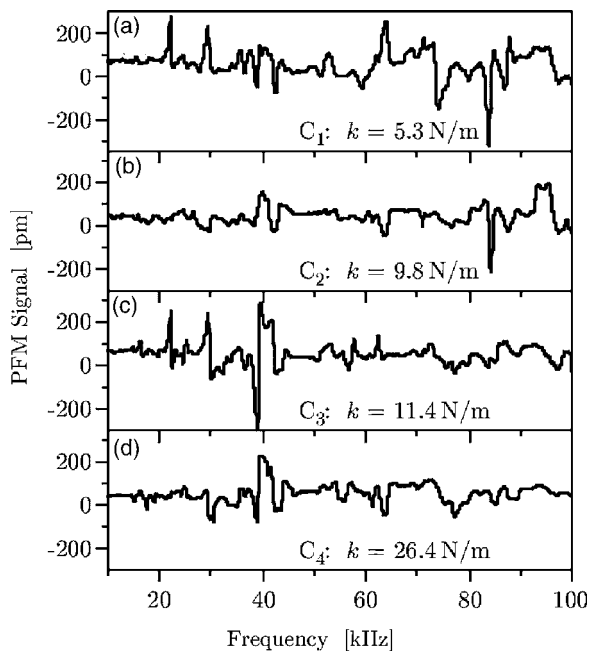


FIG. 1. Frequency dependence of the in-phase PFM signal on a - z domain face of PPLN for four different cantilevers C_1 - C_4 . k : spring constant.

fore eliminating the contributions of the ferroelectric properties of the sample [Fig. 2(a)]. To prove that these calculated curves are background signals we performed reference measurements with the same cantilever on a glass microscope slide [Fig. 2(b)]. The difference between the spectrum on LiNbO₃ and on glass is very small [Fig. 2(c), the vertical axis being expanded by a factor of 10]. The slight increase might be due to thermal drift during the scan time of 10 min. The noise of <5 pm and the residual peaks can be suppressed prolonging the scan time thereby, however, augmenting the drift. Even on metallized surfaces the same spectrum was observed,¹⁷ which underlines why we claim that this background signal is independent of the kind of sample used. Note that mechanical resonances of LiNbO₃ occur at much

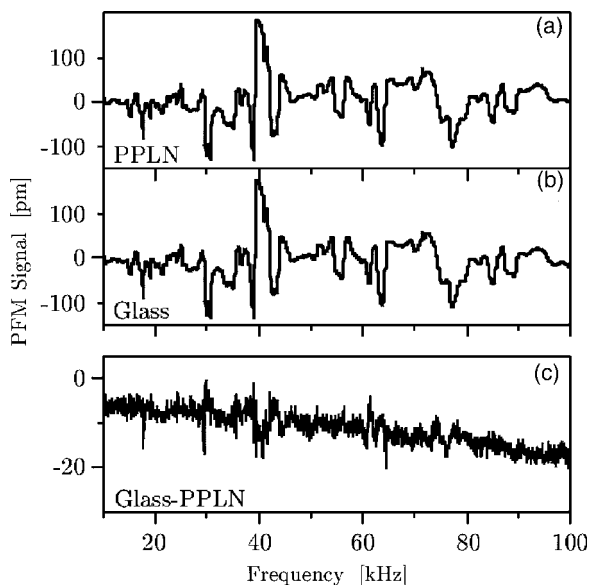


FIG. 2. Frequency dependence of the in-phase background PFM signal on a PPLN surface (a), on a glass surface (b), and their difference (c). Measurements were performed with cantilever C_4 .

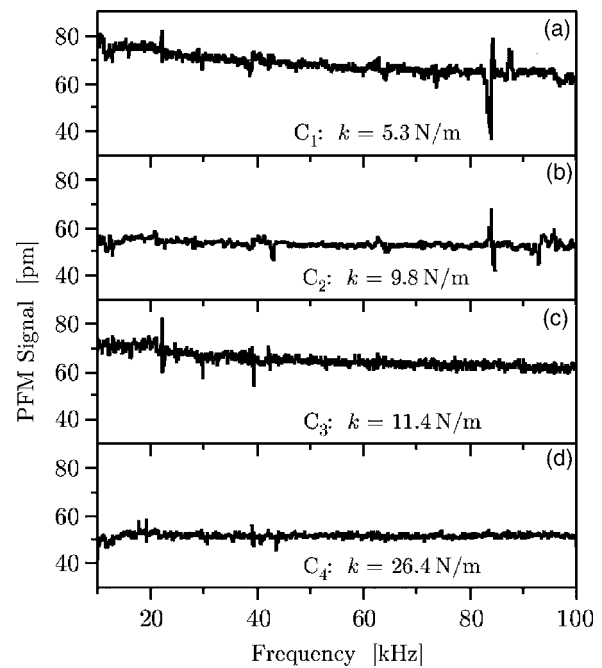


FIG. 3. Frequency dependence of the in-phase background-corrected PFM signal on a - z domain face of PPLN for four different cantilevers C_1 - C_4 . k : spring constant.

higher frequencies¹⁸ and a frequency dependence of the piezoelectric effect is known only for much lower frequencies.¹⁹

To extract the contributions of the piezoelectric properties of the LiNbO₃ sample from the PFM signal we subtracted the background from the measured data. Figure 3 shows the frequency spectra of the background-corrected X signals for the four cantilevers. They show a frequency independent spectrum; the averaged values are C_1 :62 pm, C_2 :59 pm, C_3 :71 pm, and C_4 :52 pm. This has to be compared with the theoretically expected value $\Delta t = d_{33}U = 81$ pm with $d_{33} = 8.075$ pm/V being the appropriate piezoelectric tensor element²⁰ and $U = 10$ V_{pp} the voltage applied to the tip. As expected no Y signal is obtained after background subtraction. Although the background-corrected signals are of the right magnitude, they are too small by up to 35%. A possible explanation lies in the mechanical constrictions of the deformation.⁶ The electrical field spatially decays extremely fast due to the small radius of the tip (~ 30 nm), thus thickness changes of the crystal occur in a volume comparable to the tip size. Because of its stiffness, the crystal cannot completely follow the required deformation which could be the cause for measuring too small values.

An important point here is that the corrected PFM signal was found to be independent of the stiffness of the cantilever. Additional experiments with variously coated tips (Al, Co-Cr, Cr-Au, diamond, Pt-Ir, and Ti-Pt) yield similar results too. Also varying the pressure of the tip on the sample surface by two orders of magnitude had no influence on the signals. The observed frequency spectra remain mainly unchanged. With the results described above, the contrast mechanism in PFM imaging can be fully explained through the thickness change of the sample due to the converse piezoelectric effect, taking into account the background PFM signal as determined above.

To summarize, a vector diagram illustrates the case for two different frequencies $\omega^{(1)}$ and $\omega^{(2)}$ of the alternating volt-

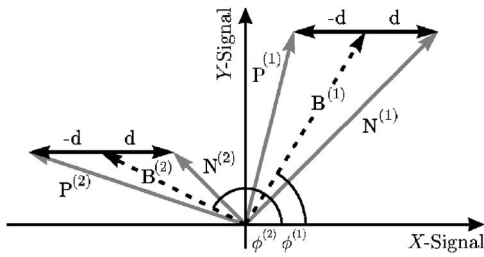


FIG. 4. Vector diagram for the domain contrast in PFM exemplified for two frequencies $\omega^{(1)}$ and $\omega^{(2)}$. The X axis denotes the in-phase output ($\theta=0^\circ$) and the Y axis the orthogonal output ($\theta=90^\circ$) of the lock-in amplifier. In the graph $\mathbf{B}^{(1)}$, $\mathbf{B}^{(2)}$ denote the background PFM signals with their corresponding phases $\phi^{(1)}$ and $\phi^{(2)}$. $\mathbf{P}^{(1)}$ and $\mathbf{P}^{(2)}$ and $\mathbf{N}^{(1)}$ and $\mathbf{N}^{(2)}$ are the measured PFM signals on $a+z$ and on a $-z$ face, respectively, and $2d$ is the domain contrast.

age (Fig. 4). At a certain frequency $\omega^{(1)}$ a background PFM signal $\mathbf{B}^{(1)}$ is present. The ferroelectric domains contribute $-d$ for the $+z$ face and $+d$ for the $-z$ face to the PFM signal, both of the same amplitude with a 180° phase shift in between. This results in the measurement of $\mathbf{P}^{(1)} = \mathbf{B}^{(1)} - d$ for the $+z$ face and $\mathbf{N}^{(1)} = \mathbf{B}^{(1)} + d$ for the $-z$ face. It is important to note that the phasing between $\mathbf{P}^{(1)}$ and $\mathbf{N}^{(1)}$ is by far not 180° ; their amplitudes are unequal and larger than expected. The same considerations apply for any other frequency $\omega^{(2)}$. It is obvious from Fig. 4 that although the domain contrast $2d$ is the same for both frequencies, the measured PFM signals differ seriously. This can be verified experimentally with an oscilloscope in X-Y-display mode when applying voltages of different frequencies to the tip while continuously scanning across a domain wall. Apart from the varying domain contrast the background can have serious consequences on the shape and the location of the domain boundaries.²¹

In conclusion we have presented a vectorial analysis of the detection mechanism of ferroelectric domains with PFM. Taking into account the background PFM signal caused by the experimental setup, basic inconsistencies in PFM measurements concerning frequency dependence, amplitude, and phasing have been removed. The domain contrast originates solely from the converse piezoelectric effect, satisfying the

generally required features of PFM imaging. The experimental data were found to be in good agreement with the theoretically expected values. Performing a quantitative analysis of the PFM signal, it can thus be determined whether an observed contrast can be attributed to the converse piezoelectric effect, therefore unambiguously proving the existence of ferroelectric domains.

The authors thank R. W. Eason for stimulating discussions. Financial support of the DFG research unit 557 and of the Deutsche Telekom AG is gratefully acknowledged.

- ¹M. M. Fejer, G. A. Magel, D. H. Jundt, and R. L. Byer, IEEE J. Quantum Electron. **28**, 2631 (1992).
- ²N. G. R. Broderick, G. W. Ross, H. L. Offerhaus, D. J. Richardson, and D. C. Hanna, Phys. Rev. Lett. **84**, 4345 (2000).
- ³Y. Cho, S. Hashimoto, N. Odagawa, K. Tanaka, and Y. Hiranaga, Appl. Phys. Lett. **87**, 232907 (2005).
- ⁴E. Soergel, Appl. Phys. B: Lasers Opt. **81**, 729 (2005).
- ⁵Nanoscale Characterisation of Ferroelectric Materials, 1st ed., edited by M. Alexe and A. Gruverman (Springer, Berlin, 2004).
- ⁶T. Jungk, Á. Hoffmann, and E. Soergel, e-print cond-mat/0607313.
- ⁷O. Kolosov, A. Gruverman, J. Hatano, K. Takahashi, and H. Tokumoto, Phys. Rev. Lett. **74**, 4309 (1995).
- ⁸L. M. Eng, H.-J. Güntherodt, G. Rosenman, A. Skliar, M. Oron, M. Katz, and D. Eger, J. Appl. Phys. **83**, 5973 (1998).
- ⁹M. Labardi, V. Likodimos, and M. Allegrini, Phys. Rev. B **61**, 14390 (2000).
- ¹⁰S. Hong, H. Shin, J. Woo, and K. No, Appl. Phys. Lett. **80**, 1453 (2002).
- ¹¹C. Harnagea, M. Alexe, D. Hesse, and A. Pignolet, Appl. Phys. Lett. **83**, 338 (2003).
- ¹²D. A. Scrymgeour and V. Gopalan, Phys. Rev. B **72**, 024103 (2005).
- ¹³A. Agronin, M. Molotskii, Y. Rosenwaks, E. Strassburg, A. Boag, S. Mutchnik, and G. Rosenman, J. Appl. Phys. **97**, 084312 (2005).
- ¹⁴J. W. Hong, K. H. Noh, S. Park, S. I. Kwun, and Z. G. Khim, Phys. Rev. B **58**, 5078 (1998).
- ¹⁵M. Shvebelman, P. Urenski, R. Shikler, G. Rosenman, Y. Rosenwaks, and M. Molotskii, Appl. Phys. Lett. **80**, 1806 (2002).
- ¹⁶S. V. Kalinin and D. A. Bonnell, Phys. Rev. B **65**, 125408 (2002).
- ¹⁷T. Jungk, Á. Hoffmann, and E. Soergel, e-print cond-mat/0602137.
- ¹⁸H. Ogi, Y. Kawasaki, M. Hirao, and H. Ledbetter, J. Appl. Phys. **92**, 2451 (2002).
- ¹⁹D. Damjanovic, Phys. Rev. B **55**, R649 (1997).
- ²⁰M. Jazbinšek and M. Zgonik, Appl. Phys. B: Lasers Opt. **74**, 407 (2002).
- ²¹T. Jungk, Á. Hoffmann, and E. Soergel, e-print cond-mat/0512373.